

Half-closed Discontinuous Galerkin discretisations

Y. Pan^{a,b,1,*}, P.-O. Persson^{a,b,2}

^a*Department of Mathematics, University of California, Berkeley, Berkeley, CA 94720, United States*

^b*Mathematics Group, Lawrence Berkeley National Laboratory, 1 Cyclotron Road, Berkeley, CA 94720, United States*

Abstract

We introduce the concept of half-closed nodes for nodal Discontinuous Galerkin (DG) discretisations. This is in contrast to more commonly used closed nodes in DG where in each element nodes are placed on every boundary. Half-closed nodes relax this constraint by only requiring nodes on a subset of the boundaries in each element, with this extra freedom in node placement allowing for increased efficiency in the assembly of DG operators. To determine which element boundaries half-closed nodes are placed on we outline a simple procedure based on switch functions. We examine the effect on operator sparsity from using the different types of nodes and show that in particular for the Laplace operator there is no difference in the sparsity from using half-closed or closed nodes. We also discuss in this work some linear solver techniques commonly used for Finite Element or Discontinuous Galerkin methods such as static condensation and block-based methods, and how they can be applied to half-closed DG discretisations.

Keywords: Discontinuous Galerkin, Sparsity, Linear solvers, Static condensation

1. Introduction

The Discontinuous Galerkin (DG) method is a popular variant of the Finite Element method which allows for allow for discontinuities between the elements in the solution space [5, 8]. Some properties of the method include its ability to easily achieve arbitrarily high orders of accuracy for a wide range of problems on unstructured meshes and to naturally allow for stabilisation through the use of approximate Riemann solvers. This has made it an attractive proposition for many fluid dynamics applications and has as a result garnered much research attention in the past few decades since its introduction by Reed and Hill [15] for the neutron transport problem.

One common criticism of the DG method however is in its cost. In addition to having extra degrees of freedom compared to continuous Finite Elements, operator assembly in DG can often be expensive as

*Corresponding author

Email addresses: y11pan@berkeley.edu (Y. Pan), persson@berkeley.edu (P.-O. Persson)

¹Graduate student, Department of Mathematics, University of California, Berkeley

²Professor, Department of Mathematics, University of California, Berkeley

numerical quadrature is necessary both inside element volumes and on their boundaries. This has led to significant research over the years leading to the development of related methods to address this such as the DG-Spectral Element Method [10], line-based DG [14], Spectral Volumes [17], Spectral Differences [12], Flux Reconstruction [9], and Hybridized Discontinuous Galerkin [2]. Many of these methods however can only be easily formulated on quadrilateral meshes, with extensions to simplex meshes often proving to be a challenge.

In this work we introduce the use of half-closed nodes in DG discretisations, which are applicable to meshes of arbitrary element shape. This is in contrast to commonly used closed nodes such as the Gauss-Lobatto or Chebyshev nodes of the second kind in DG and its related methods, where within each element nodes are placed on all its boundaries. This has the effect of creating the trademark node duplication pattern on inter-element boundaries in the DG method. Closed nodes are often chosen to ensure direct coupling between neighbouring elements and to allow for efficient computation of the boundary terms. Half-closed nodes on the other hand relax this constraint by only requiring that on each inter-element boundary between any two elements, only one of the elements must have nodes placed on that boundary. This allows for increased flexibility in node placement and we show that this simple modification can enable more efficient assembly of DG operators on both quadrilateral and simplex meshes, doing so without modifying the underlying DG formulation and its properties.

For quadrilateral elements we consider in particular using the Gauss-Radau nodes as the half-closed nodes of choice. These nodes can double as quadrature nodes for numerical integration similar to the Gauss-Lobatto nodes in the DG-Spectral Element Method, and attain an extra degree of quadrature precision over Gauss-Lobatto nodes [1]. For simplex meshes we present a novel set of half-closed approximate quadrature nodes, which with the addition of a very small number of extra quadrature points are able to attain a high degree of precision. To determine which subset of the element boundaries half-closed nodes are placed on, we introduce a simple procedure based on switch functions. The procedures for quadrilateral and simplex meshes are outlined separately to accommodate the different half-closed nodes used for each type of element.

To get a clearer picture of the cost associated with using half-closed nodes, we analyse the effect on the sparsity pattern of DG operators of using half-closed nodes for both first and second order partial differential equations. For second order equations the Local Discontinuous Galerkin (LDG) method is employed. While for first order equations a small increase in the number of non-zero entries is observed in the first derivative DG operators, the sparsity pattern when using closed or half-closed nodes is identical for second derivative operators. This suggests the possibility of commonly used linear solver techniques for DG methods using closed nodes to be applicable also to DG methods using half-closed nodes.

To this effect we discuss two types of linear solvers. The first is that of static condensation, also known as

Guyan reduction [7], popular in Finite Element methods [18]. The second is that of block-based techniques such as block-Jacobi, popular for DG methods [13]. We consider the use of these two methods in this setting and show both these techniques to in fact be readily applicable to both first and second derivative DG operators using either closed or half-closed nodes.

The paper is structured as follows. We first give a brief review of the DG method and the LDG framework for second order equations in Section 2. In Section 3, the sparsity pattern of both first and second DG operators are analysed for the different types of nodes. Specific details of half-closed nodes and their placement including the switch function construction are given in Section 4. In Section 5 we pivot to the topic of the linear solvers before finally concluding in Section 6.

2. Discontinuous Galerkin review

We briefly review the details of the Discontinuous Galerkin (DG) method. We focus here on the method applied onto first and second order equations, where in particular for second order equations we use the Local Discontinuous Galerkin (LDG) method [4]. Some resources for a more in depth discussion of the DG method include [3, 8].

2.1. Discretisation

To formulate the DG method, a domain Ω is first discretised into distinct elements $\mathcal{T}_h = \{K_n : \cup K_n = \Omega\}$. A finite element space V_h on these elements is introduced as

$$V_h = \{v_h|_K \in V(K_n)\} \tag{1}$$

where $V(K_n)$ is a function space isolated to element K_n . A popular choice for $V(K_n)$ are polynomial spaces of degree at most p which we focus on solely for this paper. For simplex elements they are commonly chosen to be the space of multivariate polynomials and for quadrilateral elements as the d -dimensional outer product of 1-dimension polynomials.

Functions in V_h are in general discontinuous along the boundaries of elements ∂K_n as functions have local support confined to a single element. Consequently numerical flux functions need to be defined on element boundaries in order to properly define the value of a function in V_h on these boundaries. Throughout the text, these numerical fluxes are denoted using hats \hat{F} , wherein the exact form of the numerical flux in general depends on the equation under consideration.

To represent the solution $u \in V_h$, a representative basis function set for $V(K_n)$ is introduced on each element, denoted $\{\phi_j\}$. A common way to do this is to on each element introduce a set of nodes s_j , and to

define an interpolatory set of functions such that $\phi_i(s_j) = \delta_{ij}$. For polynomial function spaces, the number of nodes in each element N needed to define a full set of basis functions depends on the desired polynomial order of functions in each element, and on the shape of the element itself. Specifically for a chosen polynomial order p in d -dimensions, the number of nodes required in a simplex element is $N = \binom{p+d}{d}$, whilst in quadrilateral elements is $N = (p+1)^d$.

2.2. Nodes

Nodes are commonly placed in the DG method such that N_b nodes lie on every boundary of the element so that they define a $d - 1$ -dimensional complete polynomial space of the same order p on the boundary. For polynomial function spaces in simplex elements this means that $N_b = \binom{p+d-1}{d-1}$ nodes are placed on each element boundary, whilst in quadrilateral elements $N_b = (p+1)^{d-1}$ nodes are placed on each element boundary. These are known as closed nodes, and that N_b boundary nodes are placed on all boundaries of each element results in $2N_b$ nodes on each inter-element boundary. Closed nodes are chosen usually to minimise communication across elements, as functions on element boundaries can be evaluated through only the N_b nodal values on that boundary, rather than requiring all nodal values of the element.

A less popular choice is that of open nodes, where fewer than N_b nodes are placed on all boundaries of the element. This gives extra flexibility in node placement which can allow for more efficient assembly of DG operators. The tradeoff however is that with using open nodes increased density in the off-diagonal blocks in the DG operators is generally observed, as evaluation of values on an element boundary require interpolation from all nodal values within that element.

An intermediate between these two cases is that of half-closed nodes, where N_b nodes are placed only on some boundaries of each element. Specifically half-closed nodes satisfy the constraint that on each inter-element boundary between two neighbouring elements, at least one of the elements must have N_b nodes placed on that boundary. The idea behind this is that it may allow for the retention of some of the advantages from using open or closed nodes, without incurring too much of the cost associated with strictly using one or the other. More details on how to determine which element places the N_b nodes on each inter-element boundary are given in Sect. 4.

A schematic comparing closed, open, and half-closed nodes is shown in Fig. 1. Some examples of the most popular nodes used in DG are Gauss-Lobatto, Chebyshev (both closed), Gauss-Legendre (open), and equidistant (either open or closed) nodes. Many of the above choices however are unique to quadrilateral elements however and are not easily extendable to simplex elements.

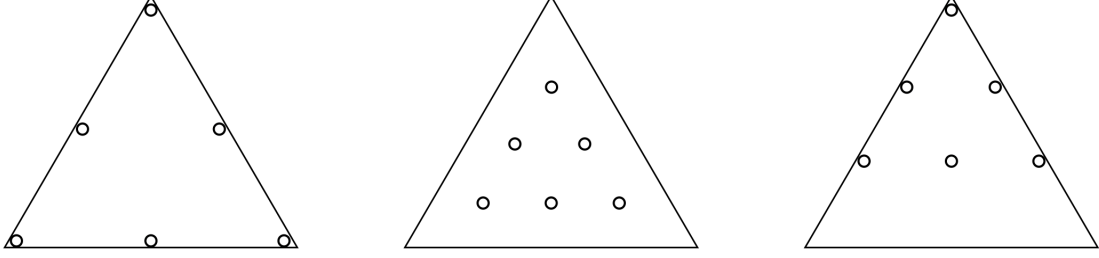


Figure 1: From left to right, examples of $p = 2$ closed, open and half-closed nodes on a simplex element.

2.3. 1st order equations

We consider the first order partial differential equation on the domain Ω with the inflow boundary denoted as Γ_{in}

$$\begin{aligned} \frac{\partial u}{\partial t} + \nabla \cdot \mathbf{F}(u) &= 0 \quad \text{in } \Omega \\ u &= g \quad \text{on } \Gamma_{\text{in}} \end{aligned} \quad (2)$$

where $\mathbf{F}(u)$ is the vector valued flux function. To find a solution $u \in V_h$, a weak formulation is obtained by multiplying Eq. 2 by a test function $v \in V_h$ and integrating by parts over each element $K_n \in \mathcal{T}_h$ to obtain

$$\frac{\partial}{\partial t} \int_{K_n} u v dx = \int_{K_n} \nabla v \cdot \mathbf{F}(u) dx - \int_{\partial K_n} v \hat{\mathbf{F}}(u) \cdot \mathbf{n} ds \quad \forall v \in V_h \quad (3)$$

where \mathbf{n} is the outward pointing normal on the boundary ∂K_n . The numerical flux $\hat{\mathbf{F}}$ is introduced only on the boundary term as boundary values of \mathbf{F} are not required for computing the volume integral. For first order equations, while many choices of numerical fluxes have been studied and used in various applications, some common choices include the Lax-Friedrich, Roe, and Godunov fluxes.

To solve this system, the solution u in K_n is expressed as a linear combination of the basis functions $u = \sum_j \phi_j u_j$, $\phi_j \in V_h$, and the test function chosen to be an arbitrary basis function $\phi_i \in V_h$. Assuming that the numerical flux can be similarly represented as a linear combination of the basis functions, substituting this in gives

$$\sum_n \int_{K_n} \phi_i \phi_j dx \cdot \frac{\partial}{\partial t} u_j = \sum_d \sum_n \int_{K_n} \frac{\partial \phi_i}{\partial x_d} \phi_j dx \cdot F_d(u_j) - \int_{\partial K_n} \phi_i \hat{\phi}_j n_d ds \cdot \hat{F}_d(u_j) \quad (4)$$

where x_d is introduced as a dummy variable for the coordinate of the d -th dimension, and $F_d(u_j), n_d$ denote the d -th component of $\mathbf{F}(u_j)$ and \mathbf{n} respectively. This can be written in operator form as

$$M \frac{\partial}{\partial t} \mathbf{u} = \sum_d D^d \mathbf{F}_d \quad (5)$$

where \mathbf{u}, \mathbf{F}_d are vectors containing the values of $u_j, F_d(u_j)$, and M, D^d are known as the mass and discrete divergence operators with entries given by

$$M_{ij} = \sum_n \int_{K_n} \phi_i \phi_j dx \quad (6)$$

$$D_{ij}^d = \sum_n \int_{K_n} \frac{\partial \phi_i}{\partial x_d} \phi_j dx - \int_{\partial K_n} \phi_i \hat{\phi}_j n_d ds \quad (7)$$

2.4. 2nd order operators

For second order equations we consider Poisson's equation

$$\begin{aligned} -\Delta u &= f \quad \text{in } \Omega \\ u &= g_D \quad \text{on } \Gamma_D \\ \nabla u \cdot \mathbf{n} &= g_N \quad \text{on } \Gamma_N \end{aligned} \quad (8)$$

as the model problem. To discretise this equation we use the LDG framework [4], which rewrites the equation into a split first order form. To do this a new variable is introduced for the gradient $\mathbf{q} = \nabla u$ and Eq. 8 is rewritten to give the new system

$$-\nabla \cdot \mathbf{q} = f \quad (9)$$

$$\mathbf{q} = \nabla u \quad (10)$$

A weak formulation is similarly obtained by multiplying this system of equations with test functions $\boldsymbol{\tau}, v$ and integrating by parts over each element K_n

$$\int_{K_n} \mathbf{q} \cdot \nabla v dx - \int_{\partial K_n} v \hat{\mathbf{q}} \cdot \mathbf{n} ds = \int_{K_n} f v dx \quad \forall v \in V \quad (11)$$

$$\int_{K_n} (\mathbf{q} + u \nabla) \cdot \boldsymbol{\tau} dx - \int_{\partial K_n} \hat{u} \boldsymbol{\tau} \cdot \mathbf{n} ds = 0 \quad \forall \boldsymbol{\tau} \in V^d \quad (12)$$

In the LDG method fluxes $\hat{u}, \hat{\mathbf{q}}$ are specified using a so-called switch function defined on the element boundary ∂K_n . For the portion of ∂K_n separating K_n and some other element K_m , the switch function is denoted S_n^m and given a value of either -1 or $+1$, where the only restriction is that $S_n^m + S_m^n = 0$. Examples of some valid switch functions are shown in Fig. 2. We consider strategies for assigning the switch function for both simplex and quadrilateral based elements in more detail in Sect. 4.

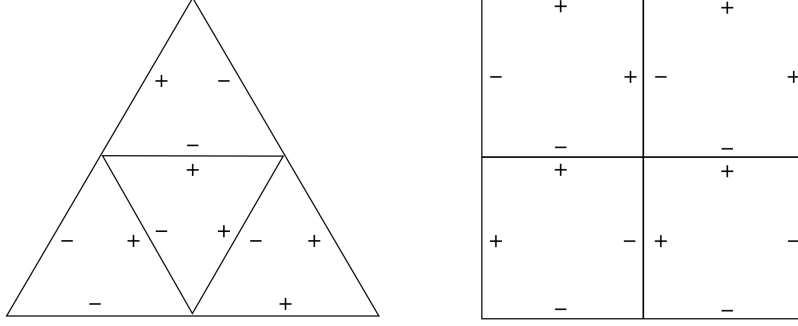


Figure 2: Example switch functions on a simplex and quadrilateral mesh in 2D. Switch function values are shown with $+$, $-$ for $+1$, -1 respectively. These switch functions are valid as the values along inter-element boundaries have opposing signs.

Given a switch function the so-called minimal dissipation LDG flux $\hat{\mathbf{q}}$ can be defined as

$$\hat{\mathbf{q}} = \begin{cases} \mathbf{q}|_{K_n} & \text{if } S_n^m < 0 \\ \mathbf{q}|_{K_m} & \text{if } S_n^m > 0 \end{cases} \quad (13)$$

and \hat{u} similarly

$$\hat{u} = \begin{cases} u|_{K_n} & \text{if } S_n^m > 0 \\ u|_{K_m} & \text{if } S_n^m < 0 \end{cases} \quad (14)$$

This is sometimes known as an upwind-downwind flux, since the value of \hat{u} , $\hat{\mathbf{q}}$ are taken from opposing elements according to the switch.

On the domain boundary, the fluxes are chosen as

$$\hat{\mathbf{q}} = \begin{cases} \mathbf{q} - C_D(u - g_D)\mathbf{n} & \text{on } \Gamma_D \\ g_N\mathbf{n} & \text{on } \Gamma_N \end{cases} \quad (15)$$

$$\hat{u} = \begin{cases} g_D & \text{on } \Gamma_D \\ u & \text{on } \Gamma_N \end{cases} \quad (16)$$

where $C_D > 0$ is a penalty parameter included for stabilisation on Dirichlet boundaries. It can be shown that the LDG method is stable with these flux definitions if the switch chosen satisfies the property that

$$\sum_{K_m \in \mathcal{N}(K_n)} |S_n^m| < |\mathcal{N}(K)|, \quad \forall K_n \in \mathcal{T}_h \quad (17)$$

where $\mathcal{N}(K_n)$ denotes the set of neighbouring elements of K_n . A switch function satisfying this property is termed a consistent switch function.

The system is solved similarly to the first order equation case by representing both u, \mathbf{q} as linear combinations of basis functions in each element, and by picking the test functions to be each of the basis functions themselves. Through this Eqs. 11 – 12 can be written in operator form as

$$\begin{bmatrix} \mathbf{M} & G \\ -D & \end{bmatrix} \begin{bmatrix} \mathbf{q} \\ u \end{bmatrix} = \begin{bmatrix} \mathbf{0} \\ f \end{bmatrix} \quad (18)$$

where \mathbf{M} is a stacked mass matrix, D the discrete divergence, and G the discrete gradient, where the gradient and divergence are related by the adjoint property $G = -D^T$. For example in two-dimensions this can be expanded to give

$$\begin{bmatrix} M & & G^x \\ & M & G^y \\ -D^x & -D^y & \end{bmatrix} \begin{bmatrix} q^x \\ q^y \\ u \end{bmatrix} = \begin{bmatrix} 0 \\ 0 \\ f \end{bmatrix} \quad (19)$$

where M is the standard mass matrix, and D^d, G^d the components of the discrete divergence and gradient. In practice the solution u can be solved for directly by taking the Schur complement of the above linear system without explicitly solving for \mathbf{q} through the system

$$-Lu = f \quad (20)$$

$$L = D^x M^{-1} G^x + D^y M^{-1} G^y \quad (21)$$

where L is known as the discrete LDG Laplacian.

3. Sparsity patterns of the operators

In this section we investigate the sparsity of the matrix operators described in the previous section. To do so we use the notation $K_n \sim K_m$ to denote neighbouring elements K_n, K_m . We examine the sparsity pattern of three operators: the mass matrix M , the discrete divergence D^d , and the discrete LDG Laplacian L . In particular we are interested in how the sparsity pattern of each operator changes when using each different type of node (open, closed, half-closed) described in Sect. 2.2.

3.1. Mass matrix

The mass matrix has entries defined in Eq. 6

$$M_{ij} = \sum_n \int_{K_n} \phi_i \phi_j dx \quad (22)$$

which contains only volume integral terms, meaning it is a block diagonal operator for any choice of nodes. This is due to the fact that the product of any two basis functions $\phi_i\phi_j \neq 0$ only if they belong to the same element.

In general for a given DG problem in d -dimensions of polynomial degree p , M is block diagonal with dense blocks of size $O(p^d)$ equal to the number of nodes and thus number of basis functions in that element. For some special choice of nodes the mass matrix can be reduced simply to a diagonal operator if

$$\sum_n \int_{K_n} \phi_i \phi_j dx = C_i \delta_{ij} \quad (23)$$

where $C_i = \sum_n \int_{K_n} \phi_i^2 dx$, that is if the basis functions are mutually orthogonal. For quadrilaterals, for any polynomial degree p examples of open nodes with this property include the Gauss-Legendre nodes and of half-closed nodes the Gauss-Radau nodes. There however do not exist any closed nodes on quadrilaterals with this property, although it is common in for instance the DG-SEM method to accept a slight under-integration and use approximate diagonal mass matrices with Gauss-Lobatto nodes. For simplices to the authors' knowledge for an arbitrary polynomial degree p there are as of yet no known nodes of any type that have this property.

3.2. Divergence/gradient operators

We examine the sparsity pattern for the divergence defined in Eq. 7 with entries given by

$$D_{ij}^d = \sum_n \int_{K_n} \frac{\partial \phi_i}{\partial x_d} \phi_j dx - \int_{\partial K_n} \phi_i \hat{\phi}_j n_d ds \quad (24)$$

and equivalently the gradient operator given they are related via a simple transpose. As with the mass matrix, the divergence operator has for each element K_n a dense block on the diagonal corresponding to the volume integral term. However this operator also has in addition an additional off-diagonal boundary integral term which depending on the exact form of the flux may couple basis functions between neighbouring elements $K_n \sim K_m$.

We consider here the sparsity of the off-diagonal blocks of the divergence operator for each of the three types of nodes separately. The communication patterns for all three types of nodes for the boundary terms of the discrete divergence operator are shown in Fig. 3. No assumptions are made on the specific form of the flux and the analysis here is for a general flux.

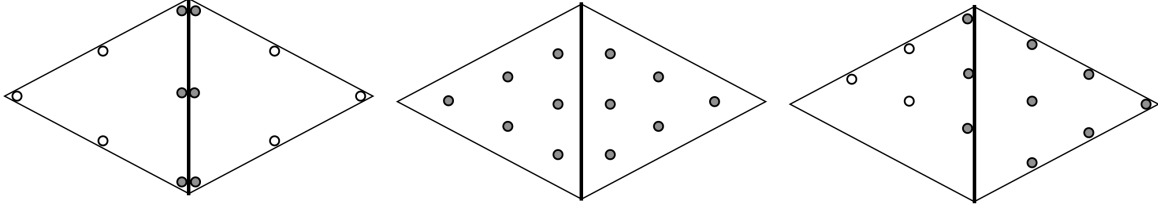


Figure 3: Communication pattern for boundary terms between neighbouring elements in discrete divergence operator for different nodes. On the left for closed nodes only the nodal values on the boundary are needed for the boundary terms. In the middle for open nodes as no nodes are on the boundary all the nodal values in both elements are needed for both elements. On the right for half-closed nodes, for the left element only the nodal values on the boundary are needed whilst on the right as no nodes are on the boundary all the nodal values in the element are needed similar to the open case.

3.2.1. Open nodes

The simplest case to consider is that of open nodes as no distinction needs to be made between nodes interior to an element and those on the boundary. In this case evaluation of function values on the boundary between $K_n \sim K_m$ requires interpolation of all nodal values from elements K_n and K_m . This in general results in a communication pattern where all nodes of elements K_n, K_m communicate with one another for the boundary integral term and implies that off-diagonal blocks in the divergence/gradient for neighbouring elements $K_n \sim K_m$ to be fully dense, with each having $O(p^{2d})$ entries.

3.2.2. Closed nodes

For closed nodes, N_b nodes are placed by each element on all its boundary such that all basis functions corresponding to interior nodes are zero on the boundaries. As a result the boundary terms in Eqs. 11 - 12 can be ignored for the interior nodes for both the divergence and gradient operators. This implies that in off-diagonal blocks corresponding to communication between neighbouring elements $K_n \sim K_m$, rows and columns corresponding to interior nodes of either K_n or K_m will not contain any non-zero entries.

Only the $2N_b$ boundary nodes from each element on the boundary between $K_n \sim K_m$ will communicate with one another for the boundary integral term in the discrete divergence and gradient. This is due to that with closed nodes the value of a function on an element boundary can always be determined using only the $2N_b$ nodal values at the boundary. Therefore the off-diagonal block in the divergence/gradient operator for neighbouring elements $K_n \sim K_m$ will each contain $O(N_b^2)$ entries, or equivalently $O(p^{2(d-1)})$ entries.

3.2.3. Half-closed nodes

In the middle is the case of half-closed nodes where on each inter-element boundary between two elements N_b nodes are required to be placed on that boundary by one of the elements. This implies that on a boundary between two elements, for at least one of the elements the values of its basis functions on that boundary are given solely by nodal values at the boundary, whilst for the other interpolation from all its nodal values may


$$\begin{pmatrix} \star & \cdot & \cdot & \cdot \\ \cdot & \star & \star & \cdot \\ \cdot & \cdot & \cdot & \cdot \\ \cdot & \cdot & \cdot & \star \end{pmatrix} \begin{pmatrix} \star & \star & \cdot & \cdot \\ \star & \star & \cdot & \cdot \\ \cdot & \cdot & \star & \star \\ \cdot & \cdot & \star & \star \end{pmatrix} = \begin{pmatrix} \star & \star & \cdot & \cdot \\ \star & \star & \star & \star \\ \cdot & \cdot & \cdot & \cdot \\ \cdot & \cdot & \star & \star \end{pmatrix}$$


Figure 4: Effect of applying an inverse mass matrix (center matrix) on the right of an arbitrary operator (left matrix). In this example the operators correspond to the two element $p = 1$ shown at the bottom. The operator initially has only one non-zero per column. After applying the mass matrix on the right this spreads the non-zero entries across the rows of each block (right matrix).

be required as with the open case. Thus the off diagonal block for neighbouring elements $K_n \sim K_m$ has at most $O(p^{2d-1})$ entries, in between that of the open and closed cases.

3.3. LDG Laplacian

The LDG Laplacian in Eq. 20 can be expressed in terms of the mass and divergence operators as

$$L = \sum_d D^d M^{-1} G^d \quad (25)$$

where now the fluxes in the divergence D^d and similarly in the gradient G^d are defined using a switch function. The only point of difference here in the gradient operators from the previous subsection is in the flux which for the divergence is now specified in Eq. 13 and for the gradient in Eq. 14. This gives that for neighbouring elements $K_n \sim K_m$ nodes from an element K_n will communicate only with nodes from K_m in the divergence operator if the switch $S_n^m > 0$. For the gradient the reverse is true due to the upwind-downwind flux structure of LDG, so that nodes from element K_n will communicate only with those from K_m if the switch $S_n^m < 0$.

From the above discussion the mass matrix is block diagonal where each block corresponds with the nodes of a single element. Furthermore the blocks are in general dense, except for some special choices of nodes described in Sect. 3.1. As such when applied to another operator on the right, the inverse mass matrix has in general the effect of spreading non-zero entries of each row out to all nodes of the element. This effect is illustrated in Fig. 4.

Since the LDG Laplacian is the sum of products of these operators, we are able to examine the sparsity patterns of the Laplacian for each type of the three nodes. We focus on the sparsity of the off-diagonal blocks as the diagonal blocks are fully dense in each of the three cases. As before each type of node is considered separately.

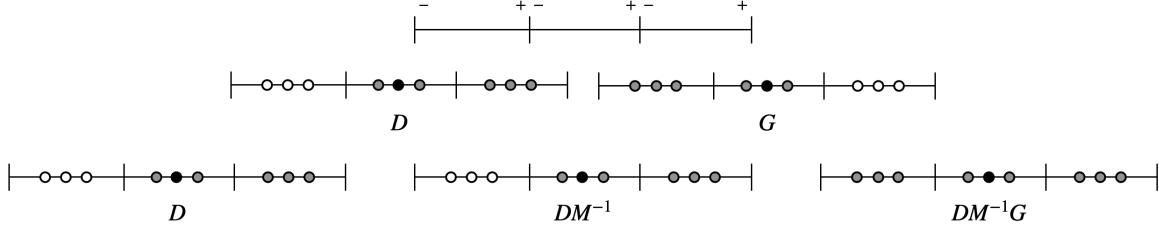


Figure 5: Communication pattern for open nodes in LDG operators on a 1D $p = 2$ mesh with switch function shown at the top. Nodes in black correspond to a node i , and shaded nodes all nodes j where the (i, j) entry of the relevant matrix is non-zero. Middle row shows divergence and gradient communication patterns for node shaded in black. On the bottom row, the operators are multiplied to give the communication pattern of the Laplacian for the node in black.

3.3.1. Open nodes

According to the switch function, for the divergence all nodes in an element K_n will communicate with those from a neighbouring element $K_n \sim K_m$ is $S_n^m > 0$. For the gradient operator the opposite is true, in that all nodes from neighbouring elements $K_n \sim K_m$ will communicate if $S_n^m < 0$. As discussed in the previous subsection for open nodes, these off-diagonal blocks are fully dense.

This means that right multiplication of the mass matrix inverse does not affect the sparsity pattern of the divergence operator in this case. The pattern can therefore be deduced by only considering the pattern of the product of the divergence with the gradient. This gives the Laplacian for open nodes will have non-zero entries in off-diagonal blocks where each node in an element K_n denoted s_j^n communicates with:

1. All nodes $\{s_j^m\}$ from neighbour elements $K_n \sim K_m$
2. All nodes $\{s_j^o\}$ from second neighbour elements $K_n \sim K_m \sim K_o$ if the switch $S_n^m < 0$ and $S_m^o < 0$

This is shown in 1D for an example mesh in Fig. 5. An example of this on a simplex mesh in 2D is also shown in Fig. 8.

3.3.2. Closed nodes

The only difference in the sparsity patterns of the divergence and gradient operators with closed nodes compared with open ones is in the sparsity of the off-diagonal blocks. In the case where closed nodes are used, as described in the previous subsection the off-diagonal blocks are sparse and only contain non-zero entries corresponding to communication between the $2N_b$ nodes on the boundary between neighbouring elements $K_n \sim K_m$. This is in contrast to the off-diagonal blocks when using an open nodes where they are fully dense.

However to compute the Laplacian matrix the divergence operator is first multiplied on the right by the inverse mass matrix. This multiplication on the right of the mass inverse to the divergence has the effect of spreading non-zero entries as shown in Fig. 4. This is then multiplied on the right by the gradient operator

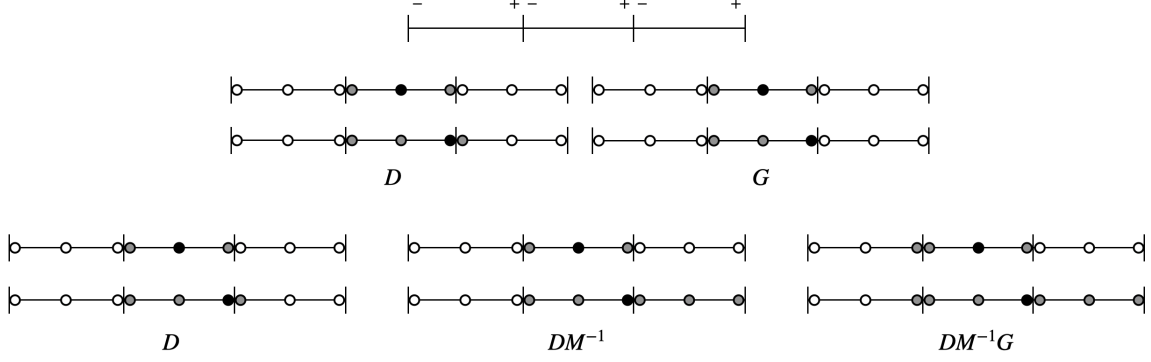


Figure 6: Communication pattern for closed nodes in LDG operators on a 1D $p = 2$ mesh for switch function shown at the top. Nodes in black correspond to a node i , and shaded nodes all nodes j where the (i, j) entry of the relevant matrix is non-zero. Middle rows shows divergence and gradient communication patterns for interior and boundary nodes shaded in black. On the bottom row, the operators are multiplied to give the communication pattern of the Laplacian for the nodes in black.

to form the LDG Laplacian. Overall this gives that the Laplacian with closed nodes has non-zero entries corresponding to communication by nodes s_j^n in element K_n with:

1. All boundary nodes $\{s_j^m\}$ from neighbour elements $K_n \sim K_m$ where $K_n^m < 0$
2. All nodes $\{s_j^m\}$ from neighbour element $K_n \sim K_m$ if $K_n^m > 0$ and the node s_j^n is on the boundary between K_n, K_m
3. All boundary nodes $\{s_j^o\}$ of second neighbour elements $K_n \sim K_m \sim K_o$ if the switch function satisfies $S_n^m < 0, S_m^o < 0$, and the node s_j^n is on the boundary between K_n, K_m

This is shown in 1D for an example mesh in Fig. 6. An example of this on a simplex mesh in 2D is also shown in Fig. 8.

3.3.3. Half-closed nodes

We make the observation that the differences in sparsity pattern of the Laplacian in the open and closed cases can be attributed simply to having N_b boundary nodes on the boundary $K_n \sim K_m$ in element K_n where the switch function satisfies $K_n^m > 0$. This suggests the following strategy for placing half-closed nodes: on an inter-element boundary between two elements $K_n \sim K_m$, element K_n must place N_b nodes on that boundary if $S_n^m > 0$, and vice versa. As the switch function is constrained to satisfy $S_n^m + S_m^n = 0$, this guarantees at least one element on each inter-element boundary will place N_b nodes on that boundary. If half-closed nodes are placed in this fashion, despite that the divergence and gradient operators have a slightly increased number of entries in off-diagonal blocks than in the closed case, the resulting sparsity pattern of the LDG Laplacian for half-closed nodes will be identical to that of closed nodes.

This in fact holds true for both simplex and quadrilateral elements. An example of the communication pattern is shown for half-closed nodes in 1D in Fig. 7. A comparison of this on simplex meshes for all three

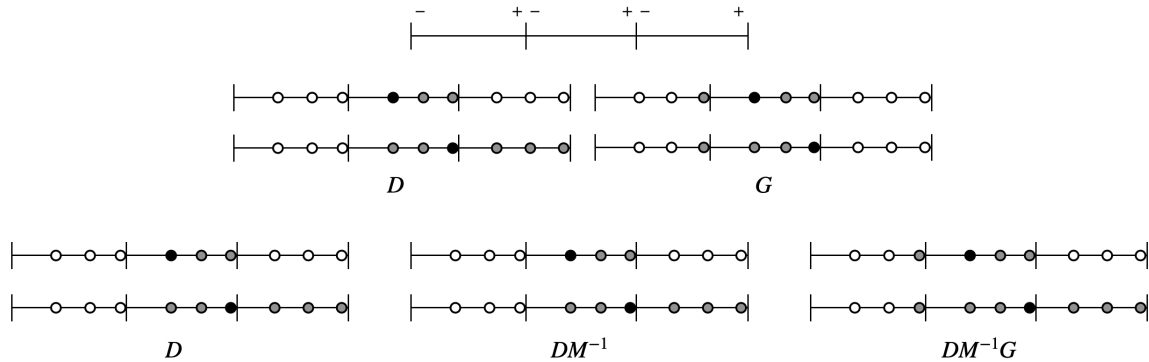


Figure 7: Communication pattern for half-closed nodes in LDG operators on a 1D $p = 2$ mesh for switch function shown at the top. Nodes in black correspond to a node i , and shaded nodes all nodes j where the (i, j) entry of the relevant matrix is non-zero. Middle rows shows divergence and gradient communication patterns for interior and boundary nodes shaded in black. On the bottom row, the operators are multiplied to give the communication pattern of the Laplacian for the nodes in black.

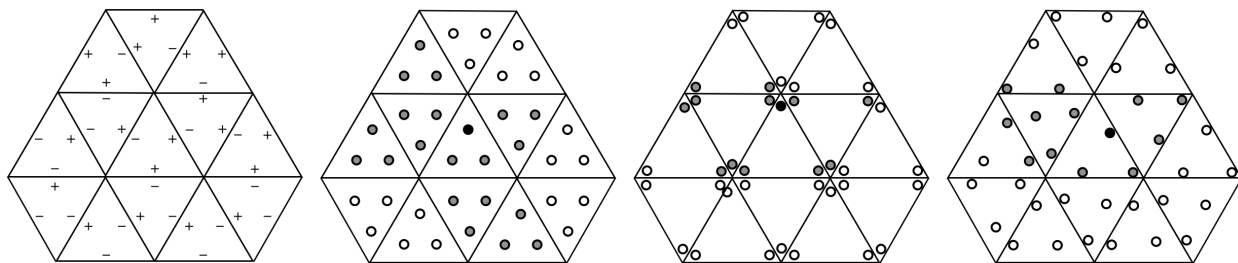


Figure 8: Communication pattern in LDG Laplacian on a 2D $p = 1$ simplex mesh for the switch function shown at the left. The number of boundary nodes to define a complete polynomial space in this case is $N_b = 2$. Nodes shaded in black correspond to a node i , and shaded nodes all nodes j where the (i, j) entry of the relevant matrix is non-zero. From middle left to the right open, closed and half-closed nodes are shown. We note that as long as N_b nodes are placed on element boundaries where the switch $S_n^m > 0$ is positive the communication patterns when using closed and half-closed nodes are identical.

types of nodes in 2D is shown also in Fig. 8.

4. Half-closed discontinuous Galerkin methods

As shown in the previous section, half-closed and closed nodes produce operators with increased sparsity compared to those with open nodes. While for first order operators operators on meshes with half-closed nodes have slightly denser off-diagonal blocks than on closed meshes, following the discussion in Sect. 3.3 if half-closed nodes are placed carefully the sparsity of second order LDG Laplace operators is identical for meshes with half-closed or closed nodes. Specifically this is achieved with half-closed nodes if for a given mesh with an assigned switch function, N_b nodes are placed on boundaries of an element K_n where the switch function $S_n^m > 0$.

One major advantage of using half-closed nodes over closed nodes is in the extra freedom with which nodes can be placed on each element, without the constraint of needing exactly N_b nodes on every element boundary unlike with closed nodes. We show that with this increased flexibility in picking nodes, more efficient assembly of the three operators in Sect. 3 can be achieved through the numerical quadrature

properties of some choices half-closed nodes. Moreover in certain cases, a sparser mass matrix can be obtained when using half-closed nodes compared to closed ones.

We discuss in this section details of half-closed nodes on both simplex and quadrilateral meshes. The two element types are considered separately. For each element type we also consider here the problem of assigning valid switch functions, as they are key to the placement of half-closed nodes.

4.1. Quadrilateral elements

4.1.1. Gauss-Radau nodes

In 1-dimension with n points on some interval, it is well known that the highest possible quadrature precision is attained through using the Gauss-Legendre points which is able to integrate exactly polynomials of degree up to $2n - 1$. The Gauss-Legendre points are however open since none of the points lie on the boundary. If the restriction is added so that nodes lie on both boundaries of the interval, that is if they are to be closed, the highest possible quadrature precision is attained through using the Gauss-Lobatto points, which integrates polynomials up to degree $2n - 3$ exactly.

If a looser restriction of only being half-closed is instead allowed, the highest possible quadrature precision is $2p - 2$ which is achieved by the Gauss-Radau points. This implies that for a given polynomial degree p , if the $p + 1$ half-closed nodes in each element in 1D are placed at the Gauss-Radau points, the integral terms in each of the operators in Sect. 3 can be computed exactly using only the nodal values of each element without requiring the usual assembly procedure of interpolating nodal values to ones at separate quadrature points. This in particular implies that in this case the mass matrix when using Gauss-Radau nodes is in fact diagonal, as opposed to only being block diagonal.

In higher dimensions, the half-closed nodes can be simply taken to be the d -dimensional outer product of the Gauss-Radau nodes in 1-dimension. This is shown on the top row of Fig. 9. Similar to 1-dimension, these nodes can be used as quadrature points to integrate d -dimensional outer products of degree at most $2p - 2$ polynomials exactly. This in particular implies that the mass matrix will remain diagonal as with the 1-dimensional case. Moreover if the boundaries of an element K_n are linear, the nodal values can be used also to calculate both the volume integral terms and the boundary integral terms without requiring any interpolation to separate boundary quadrature points.

One thing to note when using Gauss-Radau nodes is that for opposing boundaries in an element only one of them will have N_b nodes placed on it. This is a consequence of the 1-dimensional Gauss-Radau points having a boundary point on only one of the endpoints. Given that in our methodology boundary nodes in the half-closed nodes are placed according to a given switch function we therefore require a way to assign switch functions on quadrilateral meshes that satisfy the property of having opposite values for opposing

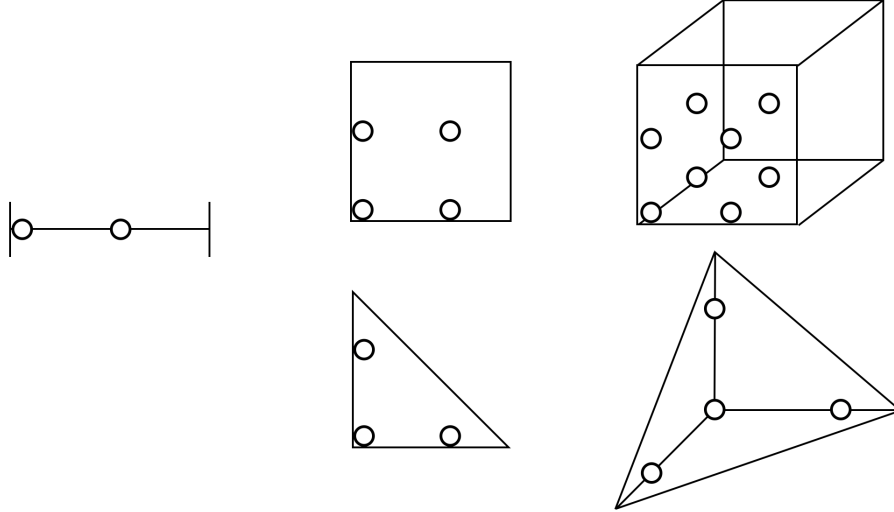


Figure 9: $p = 1$ half-closed nodes in 1D, 2D and 3D. For quadrilateral elements N_b boundary nodes are placed on 2^{d-1} boundaries whilst for simplex elements on $d - 1$ boundaries.

boundaries.

4.1.2. Switch function

To assign a valid switch function on a quadrilateral mesh, we adopt the simple algorithm used in [14]. This algorithm is constructed using the fact that switch functions on quadrilateral elements should satisfy the two properties:

1. The switch on a shared boundary between neighbouring elements $S_n \sim S_m$ should have opposing signs, that is $S_n^m + S_m^n = 0$
2. The switch on opposing boundaries in the same element should have opposing signs

Switch functions on quadrilateral elements can therefore be generated using a simple iterative algorithm, where at each step an arbitrary boundary between two neighbouring elements $S_n \sim S_m$ is picked and the switch arbitrarily assigned as $S_n^m = -1$. The two properties listed above then propagate the switch in an alternating pattern along a sequence of boundaries in both directions until either a domain boundary is reached or the sequence repeats. This procedure can then be repeated until all boundaries have been processed.

It is clear that switch functions generated via this procedure is guaranteed to satisfy the two above properties and a schematic of this procedure on a mesh in 2-dimensions is shown in Fig. 10. This is a simple consequence of the fact that at each step of the algorithm the switch is propagated by using the two properties themselves. Once a switch function has been chosen on a mesh in this way, Gauss-Radau nodes can be placed on each element K_n with boundary nodes placed according to where the switch function

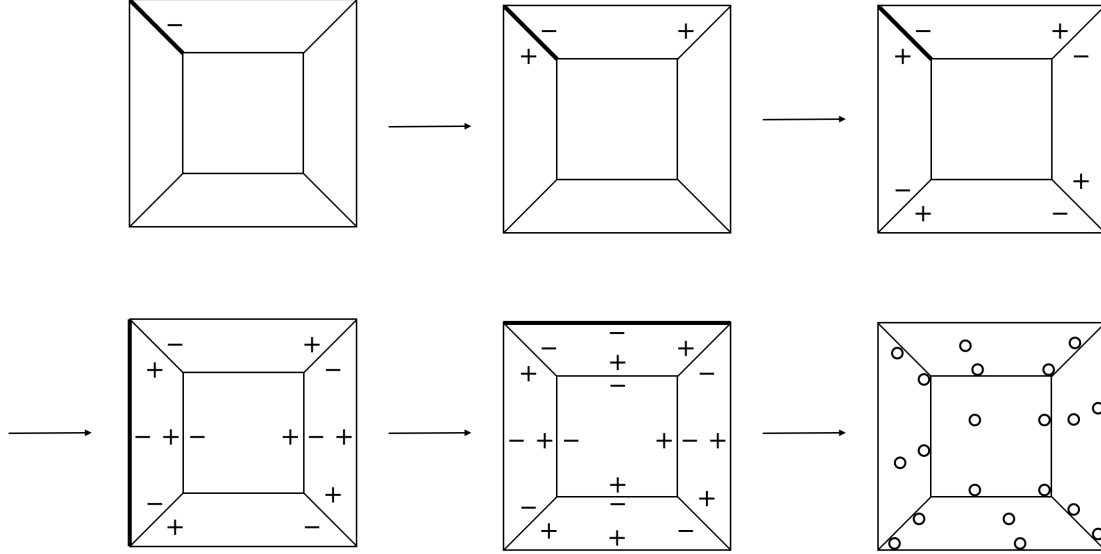


Figure 10: Schematic of switch function and node assignment on quadrilateral meshes. At each step an interior boundary between two elements shown bolded is picked and a switch of -1 arbitrarily assigned to one of the elements. This switch is then propagated in alternating fashion and the process repeated until all switches have been assigned. Finally half-closed nodes are placed in each element according to the switch function with N_b boundary nodes placed where the switch has value $+1$.

$$S_n^m > 0.$$

4.2. Simplex elements

4.2.1. Maximal approximate quadrature nodes

As described in Sect. 2.1 the number of nodes required on a simplex to define a polynomial of degree p is equal to $N = \binom{p+d}{d}$. However for $p \geq 3$ in 2-dimensions, and for $p \geq 2$ in 3-dimensions the minimum number of quadrature points required to exactly integrate a degree $2p$ polynomial is greater than the number of nodes N in a degree p simplex element [6, 19]. Furthermore these optimal quadrature rules all do not place any points on the boundaries and are as a result strictly open.

This implies that on simplex elements for there to be no analogues of the half-closed Gauss-Radau nodes or the open Gauss-Legendre nodes. Unlike in quadrilaterals there unfortunately do not exist on simplices any nodal discretisation that can integrate the mass matrix exactly for arbitrarily high polynomial degrees p , unless extra interpolation is employed to a separate set of quadrature points. In particular this means that the mass matrices produced on simplex elements will in general not be diagonal.

We instead look to place nodes in such a way that minimises the assembly cost of the derivative operators, namely the divergence, gradient and Laplacian operators. Assuming linear boundaries, the volume terms for these operators require one degree lower quadrature precision of $2p - 1$ compared to that of the mass matrix. However it turns out that even with this reduction there does not exist a set of N nodes that for arbitrarily high polynomial degree p can both be used for the nodal discretisation and attain the required

precision. Therefore instead given a degree p element we look for a maximal set of half-closed approximate quadrature nodes such that the fewest number of additional extra quadrature points is needed to integrate exactly all polynomials of degree up to and including $2p - 1$.

The advantage of using half-closed over closed nodes for simplex elements is that with the increased flexibility from relaxing the requirement of having N_b nodes on every boundary, fewer additional quadrature points are needed in the half-closed than in the closed case to exactly integrate all polynomials of degree up to $2p - 1$. For instance in 2D for a $p = 3$ element, only one additional quadrature point is needed for the optimal half-closed nodes. This is in constraint to with the optimal closed nodes where eight additional points are needed.

We restrict our search to only nodes that are symmetric with respect to interchanging of the dimensions. This implies that the resulting half-closed nodes will have N_b nodes placed on exactly $d - 1$ boundaries, as shown in the bottom row of Fig. 9. Furthermore the position of these nodes is optimised for the d -dimensional integration for the volume term without regard for the $(d - 1)$ -dimensional boundary integrals. This is as in general many more quadrature points are required for volume integrals than for the boundary ones.

We search for the maximal set of half-closed approximate quadrature nodes via a nonlinear optimisation problem. The procedure is described in more detail in Appendix B. Maximal sets of approximate quadrature nodes in 2- and 3-dimensions were found for polynomial degrees $p = 1, 2, 3$ and are reported in Appendix A. For sufficiently low polynomial degree, we found that extra quadrature nodes were not needed to achieve a quadrature precision of $2p - 1$.

4.2.2. Switch function

Following the discussion above half-closed nodes on simplices are chosen such that all boundaries but one have N_b nodes placed on them. Unlike in quadrilaterals then, the switch function on simplices only require the restriction that for every element K_n , at least one of the switches $S_n^m < 0$. This is equivalent to the condition of a switch being consistent in Eq. 17 which is required for stability of the LDG method.

Any choice of consistent switch function may therefore be used on a simplex mesh. Once the switch function is assigned, to place half-closed nodes for each element K_n we select one of the boundaries where the switch $S_n^m < 0$ at random to designate as the one where no nodes are placed. Half-closed nodes may then be placed on the element such that the other boundaries on the element K_n have N_b nodes placed on them. An example of this is shown in Fig. 11. Note that as switch functions satisfy the property that $S_n^m + S_m^n = 0$, every boundary between any two neighbouring elements $K_n \sim K_m$ will have at least N_b nodes placed on it by one of the elements K_n, K_m .

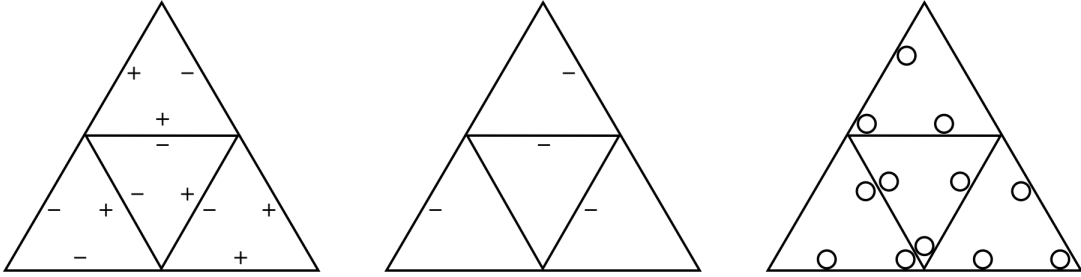


Figure 11: Half-closed node placement according to switch function in 2D simplex elements. An example switch function is shown on the left, and for each element K_n one of the boundaries where the switch $S_n^m < 0$ is selected in the middle at random. On the right half-closed nodes are placed so that nodes are placed on every boundary except those selected. Irrespective of which edge is selected in each element every boundary between any two elements will have at least $N_b = 2$ nodes placed on it.

5. Linear solvers

In this section we discuss two types of linear solver technique that aim to take advantage of the sparsity structure of the DG divergence and Laplacian operators when using half-closed nodes. We note that the constructions here can be equally applied to closed nodes, but not to open ones. This follows from the discussion of the sparsity of the operators in Sect. 3, wherein similar sparsity patterns for these operators are obtained when using closed or half-closed nodes. Specifically the sparsity pattern of the divergence operator when using a closed nodes is a strict subset of that when using a half-closed nodes, whilst for the sparsity pattern of the LDG Laplacian is identical when using either closed or half-closed nodes. Furthermore in both cases the sparsity pattern of the divergence is contained within that of the LDG Laplacian, implying that any solver technique focusing on the sparsity pattern of the Laplacian to immediately be applicable to the divergence also.

5.1. Static condensation

The first solver technique we consider is static condensation or Guyan reduction, popular in Finite Element methods (FEM). The idea behind static condensation is to via using a Schur complement eliminate a number of unknowns from a linear system, such that a smaller resultant system where the new operator has a similar sparsity pattern to the one in the original operator is obtained. For our construction here we focus on a strategy which uses the switch function to find an optimal elimination pattern within each element.

The first step of static condensation is to partition the set of nodes in a mesh into dependent and independent sets, where the dependent nodes are to be eliminated from the system. Given a linear system

$$Au = f \tag{26}$$

where A is for instance the divergence or LDG Laplace operator described in Sect. 3, the nodes are reordered such that the independent nodes are ordered first and the linear system partitioned into the form

$$\begin{bmatrix} A_{II} & A_{ID} \\ A_{DI} & A_{DD} \end{bmatrix} \begin{bmatrix} u_I \\ u_D \end{bmatrix} = \begin{bmatrix} f_I \\ f_D \end{bmatrix} \quad (27)$$

where v_I, v_D correspond to the values of a vector v for the independent and dependent nodes respectively. Assuming now that the block corresponding only to the dependent nodes A_{DD} can be easily inverted, a new reduced system can be obtained for only the independent nodes as

$$\underbrace{\left(A_{II} - A_{ID}A_{DD}^{-1}A_{DI} \right)}_{\tilde{A}} u_I = \underbrace{f_I - A_{ID}A_{DD}^{-1}f_D}_{\tilde{f}} \quad (28)$$

and we say that the dependent nodes have been eliminated, or condensed from the system. Once the solution for the independent nodes u_I has been found, the solution u_D on the dependent nodes can be easily found as the solution to

$$A_{DD}u_D = f_D - A_{DI}u_I \quad (29)$$

In particular if A_{DD} is block diagonal, the Schur complement system is extremely easy both to form and to solve. Furthermore in this case the block sparsity pattern of \tilde{A} will in fact remain to be the same as that of A_{II} . The goal therefore is to within each element find the largest possible set of dependent nodes that are eliminated such that A_{DD} remains block diagonal.

To find this set of dependent nodes, we examine the sparsity patterns of the divergence and Laplace operators. If we consider two neighbouring elements $K_n \sim K_m$, as per the discussion in Sect. 3 all nodes that do not lie on the boundary between the two elements do not communicate across elements in both operators. This implies simply that if we take the set of dependent nodes in each element K_n to be the ones not on boundaries where the switch $K_n^m > 0$, the resulting submatrix A_{DD} will be block diagonal.

For quadrilateral elements of polynomial degree p then each element can be partitioned into p^d dependent nodes to be eliminated and $(p+1)^d - p^d$ independent nodes in the reduced system. This is as in our methodology with Gauss-Radau nodes in each element exactly half the element boundaries will have boundary nodes placed on them. For simplex elements the number of dependent nodes that can be eliminated depends on the switch function in an element K_n , as unlike in quadrilateral case, the number of boundaries where the switch $S_n^m > 0$ differs from element to element.

Elimination according to this pattern guarantees that between two neighbouring elements $K_n \sim K_m$,

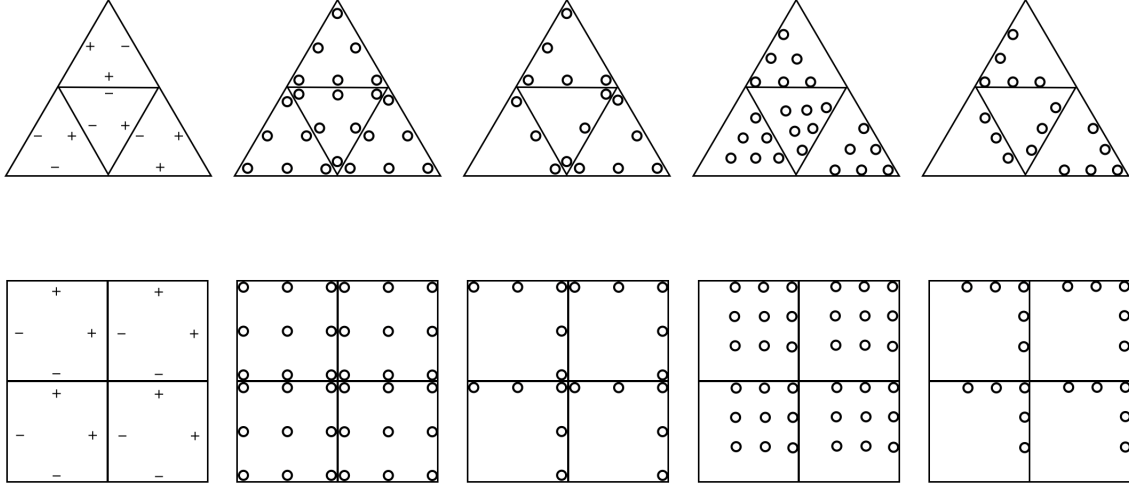


Figure 12: Static condensation elimination pattern in 2D for closed and half-closed nodes. In the left column example switch functions on quadrilateral and simplex elements are shown. In the middle column nodes not on boundaries where the switch $S_n^m > 0$ are eliminated with static condensation.

only one of the elements will have dependent nodes placed on the boundary. This is as we require the switch function to always satisfy the property $S_n^m + S_m^n > 0$. This results in the reduced mesh having only N_b boundary nodes left remaining on each boundary, which similar to that of an eliminated degree $p + 1$ FEM system of one degree higher. An example of elimination according to the switch function in 2D is illustrated in Fig. 12 on both a closed and half-closed mesh.

The idea of using static condensation for DG methods is in itself not new as has been used previously in the literature, for example in [11, 16]. The technique is also related to the hybridized discontinuous Galerkin method, [2]. However we are not aware of any elimination strategy that explicitly takes advantage of the sparsity pattern according to the switch function in this way, which allows for a greater number of dependent unknowns to be eliminated. Furthermore this strategy is easy to generalise to element of arbitrary shape, since it only requires the definition of a valid switch function.

5.2. Block solvers

A common type of solver used for DG problems are block based methods that leverage the block structure of the linear operators. These methods unlike the aforementioned static condensation can be applied on any DG method independent of the nodes used as they do not depend on the specific sparsity pattern. Popular examples of this include block Jacobi, block Gauss-Seidel and block-ILU solvers, which can either be used as a standalone method or as preconditioners or as smoothers for iterative methods.

The cost of these methods is linked directly to the size of the blocks in the DG operators. This suggests a possible efficient linear solution strategy is to first apply static condensation to reduce the number of degrees of freedom in the linear system from $O(p^d)$ to $O(p^{d-1})$ before applying standard block based solvers to solve

the reduced system. For many types of operators including the ones considered in this paper this is possible due to that taking a Schur complement of a matrix preserves many properties of linear operators. In particular important properties such as strict diagonal dominance, symmetry and positive/negative definiteness of the eigenspectrum are all preserved under the Schur complement operation.

5.3. Reduced block sizes

We can analyse more quantitatively the block sizes of the statically condensed systems by counting the number of dependent degrees of freedom eliminated via the procedure compared to the total number of degrees of freedom in the system. As the number of dependent degrees of freedom are determined solely by the switch function, this number differs from simplex to quadrilateral meshes. In particular it is found that a higher proportion of the original nodes are eliminated in general for quadrilateral meshes compared to for simplex meshes though there is no difference in the asymptotic scaling of these proportions.

5.3.1. Quadrilateral meshes

For any quadrilateral mesh in d -dimensions for a fixed polynomial degree p , the number of unknowns in the DG problem is equal to $|\mathcal{T}_h|(p+1)^d$ where $|\mathcal{T}_h|$ denotes the number of elements. Following our elimination procedure, the number of unknowns that are eliminated is always equal to $|\mathcal{T}_h|p^d$. This is due to the switch function for all quadrilaterals satisfying the property of having opposite signs on opposite boundaries in an element, and that the elimination pattern is dependent only on the switch function. As such the proportion of unknowns that are eliminated in a quadrilateral mesh is always equal to $\frac{p^d}{(p+1)^d}$.

In the simple case of Poisson's problem 1D domain $\Omega = [0, 1]$ with periodic boundary conditions we can yet analyse the effect of static condensation more precisely. Without loss of generality we can freely divide the domain into n elements of equal size with elements indexed from left to right and use the switch function given by the simple formula $S_n^m > 0$ if $n > m$ as shown in Fig. 13. For any given choice of closed or half-closed nodes, according to this switch function the nodes not on the right boundary of each element are designated as dependent nodes for the purposes of static condensation, and are eliminated from the LDG operator L via a Schur complement to give a reduced system \tilde{L} .

Remarkably for any choice of closed or half-closed nodes, the resulting reduced operator \tilde{L} has the same structure

$$\tilde{L}_{ii} = \frac{2}{h}, \quad \tilde{L}_{i,i+1} = \tilde{L}_{i+1,i} = -\frac{1}{h} \quad (30)$$

where $h = \frac{1}{n}$ is the length of each element and indices are modulo system size. This is of course the well known centred Finite Difference approximation of the second derivative and this reduced \tilde{L} is in fact obtained all polynomial orders p . While unusual this result is however perhaps not entirely unexpected; as the result



Figure 13: Static condensation for 1D example. Dependent nodes not on the boundary where the switch function $S_n^m > 0$ is positive are eliminated to give a reduced operator on the remaining independent nodes.

of a Schur complement on L the reduced operator \tilde{L} must remain a symmetric positive definite Laplacian operator on the remaining independent nodes where the sparsity pattern limits nodes of any element to communicating only with those of its immediate neighbours. As in this 1-dimensional case the independent nodes in the static condensation are independent of the initial choice of closed or half-closed nodes, it follows the reduced operator \tilde{L} is the same for any choice of these nodes.

5.3.2. Simplex meshes

For a simplex mesh in d -dimensions for a fixed polynomial degree p , the number of unknowns in a DG formulation is equal to $|\mathcal{T}_h| \binom{p+d}{d}$ where $|\mathcal{T}_h|$ denotes the number of elements. However unlike with quadrilateral meshes, the number of unknowns eliminated with static condensation varies from element to element depending on its assigned switch function. Thus the exact number of nodes to be eliminated is problem dependent, specifically on the mesh and switch function used. However on a given mesh if assuming each boundary of an element to be equally likely to be assigned a switch of ± 1 , we are able to instead calculate an expected number of eliminated variables for a given polynomial degree p .

In 2D there are only two possibilities for a valid switch function assigned to a given element. In the first case two of its boundaries are assigned a switch of $+1$ with the remaining boundary assigned -1 , whilst in the second case the reverse is true; these two configurations should be equally likely by assumption. Furthermore as shown in Fig. 12 it is easy to see that in each case, the number of dependent unknowns to be eliminated in each element K_n is equal to $\binom{p-b+d}{d}$ where b is the number of boundaries with a $S_n^m = +1$ switch assigned. This gives the expected proportion of degrees of freedom eliminated in 2D simplex mesh to be equal to $\frac{p^2}{(p+1)(p+2)}$.

The case 3D is slightly more complicated, in that there are three possible valid switch functions that may be assigned to a given element K_n . In the first case three of the four boundaries are assigned with a switch value of $S_n^m = +1$, in the second case two of the boundaries, and in the third and final case only one of the boundaries assigned this switch. By a simple counting argument it follows that each of these cases are assigned with probability $\frac{2}{7}$, $\frac{3}{7}$, $\frac{2}{7}$ respectively. Similar to the 2D case it can be seen that the number of dependent unknowns to be eliminated in each element is equal to $\binom{p-b+d}{d}$ where b is the number of boundaries with a $S_n^m = +1$ switch assigned. Altogether then for an arbitrary 3D simplex mesh this gives the expected proportion of degrees of freedom eliminated by static condensation to be equal to $\frac{7p^3+5p}{7(p+1)(p+2)(p+3)}$.

6. Conclusion

We have in this work introduced the concept of half-closed Discontinuous Galerkin discretisations, in which half-closed nodes are used to construct the nodal DG basis. For quadrilateral meshes we focus on the use of the Gauss-Radau nodes, which for straight sided elements give a diagonal mass matrix. For simplex meshes we have introduced a set of half-closed approximate quadrature nodes, which with the addition of a small number of quadrature points are able to compute the numerical integration necessary for assembling the DG derivative operators. It was found that using these nodes does not increase the number of non-zero entries in DG operators significantly when compared to using closed nodes, and in the case of the Laplace operator to not increase it at all. Moreover we showed some of the popularly used linear solver techniques for Finite Element and Discontinuous Galerkin methods to be easily applicable to half-closed DG discretisations.

For future work we plan to apply the method on a range of test problems to measure more quantitatively how properties described in this work may translate to practical speedups. Another major avenue of interest is in exploring whether the extra degree of quadrature precision attained by the Gauss-Radau nodes in quadrilateral meshes provides any advantages in avoiding aliasing issues for nonlinear problems. Finally there is also the question of whether there exists a better nodes on simplices, such that some of the properties from using Gauss-Radau nodes on quadrilaterals might transfer over.

Acknowledgments

The authors are grateful to Will Pazner for discussions which helped provide the inspiration for this work. This work was supported in part by the Director, Office of Science, Office of Advanced Scientific Computing Research, U.S. Department of Energy under Contract No. DE-AC02-05CH11231, and in part by the National Science Foundation under Grant DMS-2309596.

References

- [1] M. Abramowitz and I. A. Stegun. *Handbook of Mathematical Functions with Formulas, Graphs, and Mathematical Tables*. Dover, 9th edition, 1972.
- [2] Bernardo Cockburn, Jayadeep Gopalakrishnan, and Raytcho Lazarov. Unified hybridization of discontinuous galerkin, mixed, and continuous galerkin methods for second order elliptic problems. *SIAM Journal on Numerical Analysis*, 47(2):1319–1365, 2009.
- [3] Bernardo Cockburn, George E Karniadakis, and Chi-Wang Shu. *Discontinuous Galerkin methods: theory, computation and applications*, volume 11. Springer Science & Business Media, 2012.
- [4] Bernardo Cockburn and Chi-Wang Shu. The local discontinuous galerkin method for time-dependent convection-diffusion systems. *SIAM J. Numer. Anal.*, 35(6):2440–2463, 1998.
- [5] Bernardo Cockburn and Chi-Wang Shu. Runge-Kutta discontinuous Galerkin methods for convection-dominated problems. *J. Sci. Comput.*, 16(3):173–261, 2001.
- [6] D. A. Dunavant. High degree efficient symmetrical Gaussian quadrature rules for the triangle. *Internat. J. Numer. Methods Engrg.*, 21(6):1129–1148, 1985.
- [7] Robert J Guyan. Reduction of stiffness and mass matrices. *AIAA journal*, 3(2):380–380, 1965.
- [8] Jan S Hesthaven and Tim Warburton. *Nodal discontinuous Galerkin methods: algorithms, analysis, and applications*. Springer Science & Business Media, 2007.
- [9] Hung T Huynh. A flux reconstruction approach to high-order schemes including discontinuous galerkin methods. In *18th AIAA Computational Fluid Dynamics Conference*, page 4079, 2007.
- [10] David A Kopriva and John H Kolas. A conservative staggered-grid chebyshev multidomain method for compressible flows. *Journal of Computational Physics*, 125(1):244–261, 1996.
- [11] Wojciech Laskowski, Andrés M. Rueda-Ramírez, Gonzalo Rubio, Eusebio Valero, and Esteban Ferrer. Advantages of static condensation in implicit compressible Navier-Stokes DGSEM solvers. *Comput. & Fluids*, 209:104646, 17, 2020.
- [12] Yen Liu, Marcel Vinokur, and Zhi Jian Wang. Spectral difference method for unstructured grids i: Basic formulation. *Journal of Computational Physics*, 216(2):780–801, 2006.
- [13] P.-O. Persson and J. Peraire. Newton-GMRES preconditioning for discontinuous Galerkin discretizations of the Navier-Stokes equations. *SIAM J. Sci. Comput.*, 30(6):2709–2733, 2008.

- [14] Per-Olof Persson. A sparse and high-order accurate line-based discontinuous galerkin method for unstructured meshes. *Journal of Computational Physics*, 233:414–429, 2013.
- [15] William H Reed and Thomas R Hill. Triangular mesh methods for the neutron transport equation. Technical report, Los Alamos Scientific Lab., N. Mex.(USA), 1973.
- [16] Andres M Rueda-Ramirez, Esteban Ferrer, David A Kopriva, Gonzalo Rubio, and Eusebio Valero. A statically condensed discontinuous galerkin spectral element method on gauss-lobatto nodes for the compressible navier-stokes equations. *Journal of Computational Physics*, 426:109953, 2021.
- [17] Zhi Jian Wang. Spectral (finite) volume method for conservation laws on unstructured grids. basic formulation: Basic formulation. *Journal of Computational Physics*, 178(1):210–251, 2002.
- [18] W. Weaver and P.R. Johnston. *Structural Dynamics by Finite Elements*. Prentice-Hall civil engineering and engineering mechanics series. Prentice-Hall, 1987.
- [19] F.D. Witherden and P.E. Vincent. On the identification of symmetric quadrature rules for finite element methods. *Computers & Mathematics with Applications*, 69(10):1232–1241, 2015.

Appendix A. Simplex nodes

Half-closed approximate quadrature nodes for 2D simplices are listed here for polynomial degrees $p = 1, 2, 3$. In each case the quadrature rules have a precision of $2p - 1$. For $p = 1, 2$, no extra quadrature points are needed to attain this precision whilst for $p = 3$, one extra quadrature point is needed.

Appendix A.1. 2-dimensions

$p = 1$	x	y	w
	0	0	0
	0	2/3	1/4
Nodes	2/3	0	1/4

Table A.1: Maximal sets of half-closed approximate quadrature nodes for $p = 1$ simplex in 2D. Integration rule is exact for polynomials of degree ≤ 1 . In this case no extra quadrature points are needed.

$p = 2$	x	y	w
	0	0	0.00277069087199
	0.35505102572168	0	0.08412782572641
	0.95191835884531	0	0.03427849550426
	0	0.35505102572168	0.08412782572641
	0	0.95191835884531	0.03427849550426
Nodes	2/5	2/5	25/96

Table A.2: Maximal sets of half-closed approximate quadrature nodes for $p = 2$ simplex in 2D. Integration rule is exact for polynomials of degree ≤ 3 . In this case no extra quadrature points are needed.

$p = 3$	x	y	w
	0	0	-0.04974303679665
	0.04550534044409	0	0.04267135874628
	0.53187990947051	0	0.03619863360928
	0.96046829177904	0	0.01071791203023
	0	0.04550534044409	0.04267135874628
	0	0.53187990947051	0.03619863360928
	0	0.96046829177904	0.01071791203023
	0.25232600860719	0.25232600860719	0.14417502311789
	0.19581221710619	0.66133064003667	0.09898407391577
Nodes	0.66133064003667	0.19581221710619	0.09898407391577
Extra	0.49094860893357	0.49094860893357	0.02842405707564

Table A.3: Maximal sets of half-closed approximate quadrature nodes for $p = 3$ simplex in 2D. Integration rule is exact for polynomials of degree ≤ 5 . In this case one extra quadrature point is needed to reach the desired precision.

Appendix A.2. 3-dimensions

Half-closed approximate quadrature nodes for 3D simplices are listed here for polynomial degrees $p = 1, 2, 3$. In each case the quadrature rules have a precision of $2p - 1$. For $p = 1$, no extra quadrature points

are needed to attain this precision whilst for $p = 2$ one additional quadrature point is required and for $p = 3$, four additional quadrature points are needed.

$p = 1$	x	y	z	w
	0	0	0	1/60
	5/6	0	0	1/20
	0	5/6	0	1/20
Nodes	0	0	5/6	1/20

Table A.4: Maximal sets of half-closed approximate quadrature nodes for $p = 1$ simplex in 3D. Integration rule is exact for polynomials of degree ≤ 1 . In this case no extra quadrature points are needed to attain this precision.

$p = 2$	x	y	z	w
	0	0	0	0.00026257409675
	0.37977394053404	0	0	0.00941920026829
	0.87630759144763	0	0	0.00542514018747
	0	0.37977394053404	0	0.00941920026829
	0	0.87630759144763	0	0.00542514018747
	0	0	0.37977394053404	0.00941920026829
	0	0	0.87630759144763	0.00542514018747
	0.49448258476310	0.49448258476310	0	0.01148720843395
	0.49448258476310	0	0.49448258476310	0.01148720843395
Nodes	0	0.49448258476310	0.49448258476310	0.01148720843395
Extra	0.25140256948670	0.25140256948670	0.25140256948670	0.08740944590075

Table A.5: Maximal sets of half-closed approximate quadrature nodes for $p = 2$ simplex in 3D. Integration rule is exact for polynomials of degree ≤ 3 . In this case one extra quadrature point is needed to attain this precision.

Appendix B. Nonlinear optimisation for simplex nodes

The quadrature weights w_i and point locations $p_i = (x_i, y_i, z_i)$ in Appendix A were found via nonlinear optimisation. The setup is that of a multivariate root finding problem, with the objective function chosen such that each component of its output matches the quadrature rule with the integral of a single monomial term over a reference simplex T . In 2- and 3- dimensions the reference simplex T is taken to be the triangle and tetrahedron with edges of unit length along each of the Cartesian axes.

Symmetry constraints that the quadrature points are introduced so that the resulting quadrature rule is invariant to interchanging of the dimensions. This is achieved by removing from the system unknowns and components of the objective function that are constrained to be equal to one another due to this symmetry. This also has the dual purpose of reducing the complexity of the optimisation problem.

As a concrete example, for $p = 1$ in 2-dimensions there are three quadrature points and their respective weights that need to be found. As N_b boundary nodes are to be placed on two boundaries, this implies that one of the points p_0 must be placed at the origin, and on point on the x-axis at $p_1 = (x_1, 0)$, and another

$p = 3$	x	y	z	w
	0	0	0	-0.00100016106614
	0.09462787766324	0	0	0.00131305007975
	0.50420733108888	0	0	0.00289204970761
	0.91391988808167	0	0	0.00129146533241
	0	0.09376274016173	0	0.00131305007975
	0	0.50578817462261	0	0.00289204970761
	0	0.90831352410677	0	0.00129146533241
	0	0	0.09376274016173	0.00131305007975
	0	0	0.50578817462261	0.00289204970761
	0	0	0.90831352410677	0.00129146533241
	0.33268553961701	0.33268553961701	0	0.00866116074511
	0.33268553961701	0	0.33268553961701	0.00866116074511
	0	0.33268553961701	0.33268553961701	0.00866116074511
	0.30479878337982	0.69425396209937	0	0.0022602923837
	0.69425396209937	0.30479878337982	0	0.0022602923837
	0.30479878337982	0	0.69425396209937	0.0022602923837
	0.69425396209937	0	0.30479878337982	0.0022602923837
	0	0.30479878337982	0.69425396209937	0.0022602923837
	0	0.69425396209937	0.30479878337982	0.0022602923837
Nodes	1/3	1/3	1/3	0.00865993983562
	0.15244715165545	0.15244715165545	0.54286654052913	0.02579378134942
	0.15244715165545	0.54286654052913	0.15244715165545	0.02579378134942
	0.54286654052913	0.15244715165545	0.15244715165545	0.02579378134942
Extra	0.15272004550871	0.15272004550871	0.15272004550871	0.02579619082407

Table A.6: Maximal sets of half-closed approximate quadrature nodes for $p = 3$ simplex in 3D. Integration rule is exact for polynomials of degree ≤ 5 . In this case four extra quadrature points are needed to attain this precision.

$p_2 = (0, y_2)$ on the y -axis. However due to the symmetry constraint, it follows that $x_1 = y_2$, and furthermore that their weights $w_1 = w_2$ are equal. As a result the optimisation problems can be formulated as finding the root of multi-component objective function

$$\left(w_0 + 2w_1 - \int_T 1 \, dA, w_0 + w_1 \cdot x_1 - \int_T x \, dA \right)$$

where the unknowns to be found are $\{w_0, w_1, x_1\}$ only. Note that as the quadrature rule is constrained to be symmetric the objective only requires two components, as the term corresponding to $\int_T y \, dA$ will be automatically satisfied.